Structural Engineering and Mechanics, Vol. 25, No. 6 (2007) 733-751
DOI: http://dx.doi.org/10.12989/sem.2007.25.6.733

Interlaminar stresses and delamination of composite laminates under extension and bending

Tien Duong Nguyen†

Hanoi University of Technology, Vietnam, N° 1, Dai Co Viet St., Hanoi, Vietnam

Dang Hung Nguyen‡

LTAS – Fracture Mechanics, University of Liège, Belgium
Institut de Mécanique et Génie Civil, Bât. B52/3, Chemin des Chevreuils 1, B-4000 Liège, Belgium

(Received March 4, 2005, Accepted September 19, 2006)

Abstract. The metis element method (Hung 1978) has been applied to analyse free edge interlaminar stresses and delamination in composite laminates, which are subjected to extension and bending. The paper recalls Lekhnitskii's solution for generalized plane strain state of composite laminate and Wang's singular solution for determination of stress singularity order and of eigen coefficients $\mathbf{C}_m$ for delamination problem. Then the formulae of metis displacement finite element in two-dimensional problem are established. Computation of the stress intensity factors and the energy release rates are presented in details. The energy release rate, G, is computed by Irwin's virtual crack technique using metis elements. Finally, results of interlaminar stresses, the three stress intensity factors and the energy release rates for delamination crack in composite laminates under extension and bending are illustrated and compared with the literature to demonstrate the efficiency of the present method.

Keywords: finite element method; interlaminar stresses; composite laminate; delamination; extension; bending.

1. Introduction

Graphite-epoxy composite materials have high strength, high stiffness and low weight. So they have been reliably used in many applications from sport articles to aerospace structures.

A mode of degradation generally observed in laminated composite structures is delamination between the composite layers. The delamination can develop during manufacture by the incomplete treatment or the introduction of foreign particle; they can result from impact damages or interlaminar stresses, which are developed from free edges or discontinuities. The extension of delamination cracks appearing on free edges of composite laminates may lead to severe safety problems of aerospace composite structures.

The experimental determination of the strength of realistic composite structures requires an

† E-mail: duongnt-dwe@mail.hut.edu.vn
‡ Professor, Ph.D., Corresponding author, E-mail: H.NguyenDang@ulg.ac.be

important preparation time and highly cost. In order to reduce the number of these tests, indispensable for the first phase, the accurate modelization of the local stress field leads to a considerable reduction of structure realization cost.

The most frequently encountered fracture types in composite laminates are the high stress concentration at free edges and the delamination. Due to its complex nature, the characterization of the interface properties and the modelization are really difficult. It involves not only geometric and material discontinuities but also inherently mixed fracture modes I, II and III.

The local and precise evaluation of interlaminar stresses and of K_i, G_i, G_{total} requires a very fine mesh of finite elements near ree edges and at the crack tip of delamination. In order to appreciably reduce the fine mesh in classical finite element types, we undertook the development of a finite element in 2 dimensions (2D) of the mongrel type in regular and singular stress fields. That is the metis finite element method. The metis displacement element is special case of the original hybrid stress element, but the boundary second field (displacement field) is unisolvent. This means that the displacement field is defined completely and continuous perfectly both within the domain, and on the boundary in such away that it is conform in the connection between elements. The unisolvent condition of the external displacement field of this type of element permits to transform the contour integral respectively to the volume integral for 3D problems and the surface integral for 2D problems (Nguyen, T.D. and Nguyen, D.H. 2004, in press, Nguyen, D.H. *et al*. 1991, De Saxce 1992, Kang 1991, Fleury 1994, De Saxce and Kang 1992). So this method has the advantages of classical pure elements and hybrid elements (Nguyen, D.H. 1978).

2. Generalized plane strain state and its solutions

Consider a rectangular multilayer laminate plate composed of orthotropic linear elastic unidirectional plies (Fig. 1(a)). The composite laminate is subjected to a loading at the ends whose nature will be specified later.

The composite laminate is assumed to be sufficiently long that, in the region far from the ends, the effects are negligible by virtue of Saint Venant's principle. Consequently, stresses in the laminate are independent of the z axis. This particular state of stress and strain is qualified generalized plane strain state

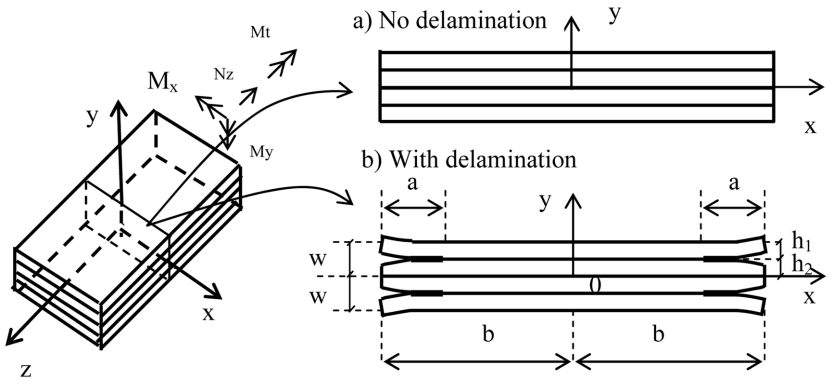

Fig. 1(a) Multilayer plate in composite materials

$$\sigma_i = \sigma_i(x, y); \quad \varepsilon_i = \varepsilon_i(x, y) \tag{1}$$

Lekhnitskii (1963) suggests that the normal strain distribution in the z direction is known and imposed by the formula

$$\varepsilon_3 = \varepsilon_z = e(x, y) \tag{2}$$

Where $e(x, y)$ is the axial strain which is independent of the z axis.

Replace Eq. (2) into the Hook's law: $\varepsilon_i = S_{ij}\,\sigma_j$ ($i, j = 1, 2, ..., 6$), σ_z has the form: $\sigma_z = (e - \sigma_\beta S_{3\beta})/S_{33}$ ($\alpha, \beta = 1, 2, 4, 5, 6$).

Eliminate σ_z from the Hooke's law, it becomes

$$\varepsilon_\alpha = S^d_{\alpha\beta}\sigma_\beta + \tilde{\varepsilon}_\alpha \text{ where } S^d_{\alpha\beta} = S_{\alpha\beta} - S_{\alpha 3}S_{3\beta}/S_{33} \text{ and } \tilde{\varepsilon}_\alpha = eS_{\alpha 3}/S_{33} \tag{3}$$

$S^d_{\alpha\beta}(\alpha, \beta = 1, 2, 4, 5, 6)$ is the reduced compliance tensor of $S_{ij}(i, j = 1, 2, ..., 6)$.

The integration of the compatibility equations gives a reduced form of the displacement field after eliminate the rigid modes

$$\begin{aligned} u^{3D}(x, y, z) &= X_3 z^2/2 + K_5 yz + u(x, y) && \text{(a)} \\ v^{3D}(x, y, z) &= -K_3 z^2/2 - K_5 xz + v(x, y) && \text{(b)} \\ w^{3D}(x, y, z) &= (-X_3 x + K_3 y + \varepsilon_3^o)z + w(x, y) && \text{(c)} \end{aligned} \tag{4}$$

Where ε_3^o is the mean strain; K_3 is the bending curvature in the weak inertia plan Oyz; X_3 is the same quantity in the strong inertia plan Oxz; K_5 is the warping angle about z-axis.

From the limited conditions, it conduits to solve the problem

$$\text{Find } \{\mathbf{u}, \boldsymbol{\varepsilon}, \boldsymbol{\sigma}\} \text{ such that: } \begin{cases} \text{(a)} \quad \boldsymbol{\varepsilon} = \mathbf{S}^d\boldsymbol{\sigma} + \boldsymbol{\varepsilon}^o \\ \text{(b)} \quad \boldsymbol{\varepsilon} = \mathbf{def}\,\mathbf{u} \\ \text{(c)} \quad \mathbf{equ}\,\boldsymbol{\sigma} = \mathbf{0} \end{cases} \text{in} \quad \Omega$$
$$\text{(d)} \quad \mathbf{t}(\boldsymbol{\sigma}) = \mathbf{0} \qquad \text{on} \quad \partial\Omega \tag{5}$$

Where **def** is the partial derivative operator of "strain"; **equ** is the partial derivative operator of "equilibrium"; $\boldsymbol{\varepsilon}^o$ is the vector of the imposed initial strains; Ω is the section of the structure; $\partial\Omega$ is the boundary of the section Ω.

$$\boldsymbol{\varepsilon}^T = [\varepsilon_1, \varepsilon_2, \varepsilon_4, \varepsilon_5, \varepsilon_6]; \quad \boldsymbol{\sigma}^T = [\sigma_1, \sigma_2, \sigma_4, \sigma_5, \sigma_6];$$
$$\varepsilon_1^o = \tilde{\varepsilon}_1, \varepsilon_2^o = \tilde{\varepsilon}_2, \varepsilon_4^o = \tilde{\varepsilon}_4 + K_5 x, \varepsilon_5^o = \tilde{\varepsilon}_5 - K_5 y, \varepsilon_6^o = \tilde{\varepsilon}_6$$
$$\mathbf{t}(\boldsymbol{\sigma}) \text{ is the tension on the boundary } \partial\Omega\text{: } \mathbf{t}(\boldsymbol{\sigma}) = \sigma_{i\alpha} n_\alpha \tag{6}$$

The equilibrium plane stress field (σ_x, σ_y, τ_{xy}) is derived from the Airy's stress function $F(x, y)$, the anti-plane stress field (τ_{xz}, τ_{yz}) from Prandtl function $\Psi(x, y)$

$$\sigma_1 = \frac{\partial^2 F}{\partial y^2}; \quad \sigma_2 = \frac{\partial^2 F}{\partial x^2}; \quad \sigma_6 = -\frac{\partial^2 F}{\partial x \partial y}; \quad \sigma_4 = -\frac{\partial \Psi}{\partial x}; \quad \sigma_5 = \frac{\partial \Psi}{\partial y} \tag{7}$$

The Beltami-Michell compatibility equations are reduced to the form (Lekhnitskii 1963)

$$L_4F + L_3\Psi = 0; \quad L_3F + L_2\Psi = 0 \tag{8}$$

Where L_2, L_3 and L_4 are derivative operators in order 2, 3 and 4, respectively.

Using the generalized complex variable $z_m = x + \mu_m y$, and its conjugated $\bar{z}_m = x + \bar{\mu}_m y$ where m = 1, 2, 3, 4, 5 and 6; and μ_m are the roots of the characteristic equation associated to the ply (Lekhnitskii 1963)

$$l_4(\mu)l_2(\mu) - l_3^2(\mu) = 0 \tag{9}$$

Where

$$l_2(\mu) = S_{55}^d\mu^2 - 2S_{45}^d\mu + S_{44}^d \quad \text{(a)}$$

$$l_3(\mu) = S_{15}^d\mu^3 - (S_{14}^d + S_{56}^d)\mu^2 + (S_{25}^d + S_{46}^d)\mu - S_{24}^d \quad \text{(b)}$$

$$l_4(\mu) = S_{11}^d\mu^4 - 2S_{16}^d\mu^3 + (2S_{12}^d + S_{66}^d)\mu^2 - 2S_{26}^d\mu + S_{22}^d \quad \text{(c)}$$

The general solution of the equation system (8) was found by Lekhnitskii (1963)

$$F = \sum_{m=1}^{3}[F_m(z_m) + F_{m+3}(\bar{z}_m)] \quad \text{(a)}; \quad \Psi = \sum_{m=1}^{3}[\eta_m F'_m(z_m) + \bar{\eta}_m F'_{m+3}(\bar{z}_m)] \quad \text{(b)} \tag{10}$$

Where $-\eta_m = -l_3(\mu_m)/l_2(\mu_m)$. The prime (') denotes differentiation of the function F.

Wang (1984) proposed a particular form of the function F for delamination problem

$$F_m(z_m) = \frac{\mathbf{C}_m z_m^{\delta+2}}{(\delta+2)(\delta+1)} \tag{11}$$

Where the stress singularity order δ is so that $-1 < \mathrm{Re}(\delta) < 0$ for singular solution so that energy is finite, where Re represents the real part of δ. The quantities $\mathbf{C}_m$ are arbitrary constants to be determined. The stress field becomes

$$\boldsymbol{\sigma} = \sum_{m=1}^{3}[\mathbf{C}_m\mathbf{r}_m z_m^{\delta} + \mathbf{C}_{m+3}\bar{\mathbf{r}}_m\bar{z}_m^{\delta}] \quad \text{where} \quad \mathbf{r}_m^T = [\mu_m^2, 1, -\mu_m, -\eta_m, \mu_m\eta_m] \tag{12}$$

From the Hooke's law and the compatible equations, the displacement field is calculated

$$\mathbf{u} = \sum_{m=1}^{3}[\mathbf{C}_m\mathbf{T}_m z_m^{\delta+1} + \mathbf{C}_{m+3}\bar{\mathbf{T}}_m\bar{z}_m^{\delta+1}]/(\delta+1) \quad \text{where} \quad \mathbf{T}_m^T = [p_m, q_m, t_m] \tag{13}$$

with

$$p_m = S_{11}^d\mu_m^2 + S_{12}^d - S_{14}^d\eta_m + S_{15}^d\eta_m\mu_m - S_{16}^d\mu_m \quad \text{(a)}$$

$$q_m = S_{21}^d\mu_m + S_{22}^d/\mu_m - S_{24}^d\eta_m/\mu_m + S_{25}^d\eta_m - S_{26}^d \quad \text{(b)}$$

$$t_m = S_{41}^d\mu_m + S_{42}^d/\mu_m - S_{44}^d\eta_m/\mu_m + S_{45}^d\eta_m - S_{46}^d \quad \text{(c)}$$

There exists 6 continuity conditions of stress and displacement vectors along the interface of two adjacent plies k and k + 1 (Fig. 1(b)) and 6 other free stress conditions on the lips of the crack to determine 12 unknowns $\mathbf{C}_m$.

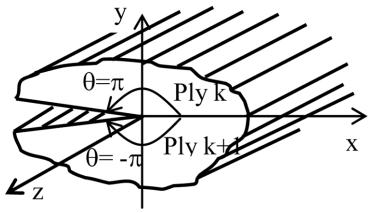

Fig. 1(b) Edge delamination between kth and $(k+1)$th plies

The 6 continuity conditions of stresses and displacements

$$\sigma_2^{(k)}\big|_{\theta=0} = \sigma_2^{(k+1)}\big|_{\theta=0}; \quad \sigma_4^{(k)}\big|_{\theta=0} = \sigma_4^{(k+1)}\big|_{\theta=0}; \quad \sigma_6^{(k)}\big|_{\theta=0} = \sigma_6^{(k+1)}\big|_{\theta=0}$$
$$u^{(k)}\big|_{\theta=0} = u^{(k+1)}\big|_{\theta=0}; \quad v^{(k)}\big|_{\theta=0} = v^{(k+1)}\big|_{\theta=0}; \quad w^{(k)}\big|_{\theta=0} = w^{(k+1)}\big|_{\theta=0}$$

The 6 free stress conditions

$$\sigma_2^{(k)}\big|_{\theta=\pi} = \sigma_4^{(k)}\big|_{\theta=\pi} = \sigma_6^{(k)}\big|_{\theta=\pi} = 0$$
$$\sigma_2^{(k+1)}\big|_{\theta=-\pi} = \sigma_4^{(k+1)}\big|_{\theta=-\pi} = \sigma_6^{(k+1)}\big|_{\theta=-\pi} = 0$$

The system of 12 equations may be written under the following form

$$\begin{bmatrix} \rho\mathbf{M}_1 & \overline{\mathbf{M}}_1 & 0 & 0 \\ 0 & 0 & \mathbf{M}_2 & \rho\overline{\mathbf{M}}_2 \\ \mathbf{M}_1 & \overline{\mathbf{M}}_1 & -\mathbf{M}_2 & -\overline{\mathbf{M}}_2 \\ \mathbf{T}_1 & \overline{\mathbf{T}}_1 & -\mathbf{T}_2 & \overline{\mathbf{T}}_2 \end{bmatrix} \begin{bmatrix} \mathbf{C}_1 \\ \mathbf{D}_1 \\ \mathbf{C}_2 \\ \mathbf{D}_2 \end{bmatrix} = \begin{bmatrix} \mathbf{0} \\ \mathbf{0} \\ \mathbf{0} \\ \mathbf{0} \end{bmatrix} \tag{14}$$

Where $\rho = e^{2i\pi\delta}$; $\mathbf{M}_m^{(k)T} = [1, \eta_m^{(k)}, \mu_m^{(k)}]$; $\mathbf{C}_k^T = [C_1^{(k)}, C_2^{(k)}, C_3^{(k)}]$;
$\mathbf{D}_k^T = [D_1^{(k)}, D_2^{(k)}, D_3^{(k)}]$; $\mathbf{M}_k = [\mathbf{M}_1^{(k)}, \mathbf{M}_2^{(k)}, \mathbf{M}_3^{(k)}]$; $\mathbf{T}_k = [\mathbf{T}_1^{(k)}, \mathbf{T}_2^{(k)}, \mathbf{T}_3^{(k)}]$

Solving the equation system (14) leads to eigen value problem. The stress singular order δ (where $\delta^T = [\delta_1, \delta_2, \delta_3]$) and the eigen coefficients C_m obtained in solving this eigen value problem.

3. Metis displacement model

In the technique of the hybrid elements of displacement, the Lagrangian of this problem is

$$\Pi(\boldsymbol{\sigma}, \mathbf{u}) = \sum_e \int_{\Omega_e} W(\boldsymbol{\sigma}) d\Omega - \sum_i \int_{S_i} \mathbf{u}^T \mathbf{t}(\boldsymbol{\sigma}) dS - \int_{\partial\Omega} \mathbf{u}^T \mathbf{t}(\boldsymbol{\sigma}) dS \quad \text{(a)}$$
$$\Pi(\boldsymbol{\sigma}, \mathbf{u}) = \sum_e \Pi_e(\boldsymbol{\sigma}, \mathbf{u}) \quad \text{(b)} \tag{15}$$

Where $$W(\boldsymbol{\sigma}) = \frac{1}{2}\boldsymbol{\sigma}^T\mathbf{S}^d\boldsymbol{\sigma} + \boldsymbol{\sigma}^T\boldsymbol{\varepsilon}^o \tag{16}$$

S_i is an interface between two contiguous elements: $\mathbf{t}(\boldsymbol{\sigma}) = \mathbf{0}$ on S_i (17)

Replace Eqs. (17) and (16) into Eq. (15), the Lagrangian of the element becomes

$$\Pi_e(\boldsymbol{\sigma}, \mathbf{u}) = \int_{\Omega_e}\left(\frac{1}{2}\boldsymbol{\sigma}^T\mathbf{S}^d\boldsymbol{\sigma} + \boldsymbol{\sigma}^T\boldsymbol{\varepsilon}^o\right)d\Omega - \int_{\partial\Omega_e}\mathbf{u}^T\mathbf{t}(\boldsymbol{\sigma})dS \tag{18}$$

The corresponding associated form of problem (5) is: $$\begin{array}{l}\underset{\mathbf{u}}{\text{Inf}}\ \underset{\boldsymbol{\sigma}}{\text{Sup}}\ \Pi(\boldsymbol{\sigma}, \mathbf{u}) \\ \mathbf{equ}\ \boldsymbol{\sigma} = \mathbf{0}\ \text{ in }\ \Omega_e\end{array} \tag{19}$$

It means that finding the maximum (Sup) of the function $\prod(\sigma, u)$ with respect to the stress field $\boldsymbol{\sigma}$ in which: $\mathbf{equ}\ \boldsymbol{\sigma} = \mathbf{0}$ in Ω_e and the minimum (Inf) of the function $\prod(\sigma, u)$ with respect to the displacement field $\mathbf{u}$.

In the metis element method, Lagrange's multiplier field, which is interpreted physically as the displacement field is prolonged to interior of each element in a continuous manner (unisolvent principle). This principle permits to transform a contour integral into volume integral or into surface integral (De Saxce 1992)

$$\int_{\partial\Omega_e}\mathbf{u}^T\mathbf{t}(\boldsymbol{\sigma})dS = \int_{\Omega_e}(\boldsymbol{\sigma}^T\mathbf{def}\ \mathbf{u} + \mathbf{u}^T\mathbf{equ}\ \boldsymbol{\sigma})d\Omega \tag{20}$$

Introducing Eq. (20) into Eq. (18) in taking account of the internal equilibrium in each element conducts to the expression following

$$\Pi_e(\boldsymbol{\sigma}, \mathbf{u}) = \int_{\Omega_e}\left(\frac{1}{2}\boldsymbol{\sigma}^T\mathbf{S}^d\boldsymbol{\sigma} + \boldsymbol{\sigma}^T\boldsymbol{\varepsilon}^o - \boldsymbol{\sigma}^T\mathbf{def}\ \mathbf{u}\right)d\Omega \tag{21}$$

All elements of the structure (E) are divided into the elements around the crack tip named singular elements (S) and the rest elements named regular elements (R)

$$E = R \cup S: \quad R \cap S = \varnothing$$

- In regular elements

Introduce the discretized displacement field $\mathbf{u} = \mathbf{N}(x)\mathbf{q}$ (where: $\mathbf{N}(x)$ is the shape function matrix of the displacement; $\mathbf{q}$ is the nodal displacement vector) and the discretized stress field $\boldsymbol{\sigma} = \mathbf{R}_R(x)\mathbf{h}_{e1}$ (where: $\mathbf{R}_R(x)$ is the polygonal interpolation matrix of regular stresses of element; $\mathbf{h}_{e1}$ is the vector of unknown parameters whose number is associated to select degree of the regular discretisation) into Eq. (21), it becomes

$$\Pi_e(\mathbf{h}_{e1}, \mathbf{q}) = \frac{1}{2}\mathbf{h}_{e1}^T\mathbf{F}_{e1}\mathbf{h}_{e1} + \mathbf{h}_{e1}^T\mathbf{v}_{e1}^o - \mathbf{h}_{e1}^T\mathbf{G}_{e1}^T\mathbf{q} \tag{22}$$

Where $\mathbf{F}_{e1} = \int_{\Omega_e}\mathbf{R}_R^T\mathbf{S}^d\mathbf{R}_R d\Omega$; $\mathbf{v}_{e1}^o = \int_{\Omega_e}\mathbf{R}_R^T\boldsymbol{\varepsilon}^o d\Omega$; $\mathbf{G}_{e1} = \int_{\Omega_e}\mathbf{B}^T\mathbf{R}_R d\Omega$

The variational equation of Eq. (22) with respect to $\mathbf{h}_{e1}$ gives

$$\mathbf{F}_{e1}\mathbf{h}_{e1} + \mathbf{v}_{e1}^o - \mathbf{G}_{e1}^T\mathbf{q} = \mathbf{0} \tag{23}$$

Let $\mathbf{g}_e = \mathbf{G}_{e1}\mathbf{h}_{e1}\left(= \dfrac{\partial \Pi_e}{\partial q}\right)$ called the generalized force of each element. (24)

Replacing $\mathbf{h}_{e1}$ from Eq. (23) into the formula of $\mathbf{g}_e$ in Eq. (24) gives

$$\mathbf{g}_e = \mathbf{K}_e\mathbf{q} - \mathbf{g}_e^o \quad \forall e \in R \tag{25}$$

Where $\mathbf{K}_e = \mathbf{G}_{e1}\mathbf{F}_{e1}^{-1}\mathbf{G}_{e1}^T$; $\mathbf{g}_e^o = \mathbf{G}_{e1}\mathbf{F}_{e1}^{-1}\mathbf{v}_{e1}^o$

- *In singular elements*

The displacement field has the form: $\mathbf{u} = \mathbf{N}(x)\mathbf{q}$. (26)

The stress field in singular elements contains regular part ($\boldsymbol{\sigma}^R$) and a singular part ($\boldsymbol{\sigma}^S$)

$$\boldsymbol{\sigma} = \boldsymbol{\sigma}^R + \boldsymbol{\sigma}^S = \mathbf{R}_R(x)\mathbf{h}_{e1} + \mathbf{R}_S(x)\mathbf{h}_{e2} \tag{27}$$

Where $\mathbf{R}_S(x)$ is the singular matrix defined from the singular stress field (Fleury *et al.* 1994)

$$\sigma_i = h_{e2,1}\sum_{m=1}^{3}[\mathrm{Re}(C_{m,1}r_{i,m}z_m^{\delta_1}) + \mathrm{Im}(C_{m+3,1}\bar{r}_{i,m}\bar{z}_m^{\delta_1})] +$$

$$+ h_{e2,2}\sum_{m=1}^{3}\mathrm{Re}(C_{m,2}r_{i,m}z_m^{\delta_2} + C_{m+3,2}\bar{r}_{i,m}\bar{z}_m^{\delta_2}) + h_{e2,3}\sum_{m=1}^{3}\mathrm{Im}(C_{m,3}r_{i,m}z_m^{\delta_3} + C_{m+3,3}\bar{r}_{i,m}\bar{z}_m^{\delta_3})$$

With i = 1, 2, 4, 5, 6.

$\mathbf{h}_{e2}$ is the vector of unknown parameters of singular part of discretisation stress field

$\mathbf{h}_{e2}{}^T = [h_{e2,1}, h_{e2,2}, h_{e2,3}]$.

Numerical tests showed that the better results are obtained when we identify $\mathbf{h}_{e2}$ as common nodal variables $\mathbf{h}_2$ on the common crack tip node of finite elements. Introducing these two fields into Eq. (21), it obtains

$$\Pi_e(\mathbf{h}_{e1}, \mathbf{h}_2, \mathbf{q}) = \frac{1}{2}\mathbf{h}_{e1}^T\mathbf{F}_{e1}\mathbf{h}_{e1} + \mathbf{h}_{e1}^T\mathbf{v}_{e1}^o - \mathbf{h}_{e1}^T\mathbf{G}_{e1}^T\mathbf{q} + \mathbf{h}_{e1}^T\mathbf{F}_{e12}\mathbf{h}_2 + \frac{1}{2}\mathbf{h}_2^T\mathbf{F}_{e2}\mathbf{h}_2 + \mathbf{h}_2^T\mathbf{v}_{e2}^o - \mathbf{h}_2^T\mathbf{G}_{e2}^T\mathbf{q} \tag{28}$$

Where $\mathbf{F}_{e1} = \int_{\Omega e}\mathbf{R}_R^T\mathbf{S}^d\mathbf{R}_R d\Omega$; $\mathbf{v}_{e1}^o = \int_{\Omega e}\mathbf{R}_R^T\boldsymbol{\varepsilon}^o d\Omega$; $\mathbf{G}_{e1} = \int_{\Omega e}\mathbf{B}^T\mathbf{R}_R d\Omega$;

$\mathbf{F}_{e2} = \int_{\Omega e}\mathbf{R}_S^T\mathbf{S}^d\mathbf{R}_S d\Omega$; $\mathbf{F}_{e12} = \int_{\Omega e}\mathbf{R}_R^T\mathbf{S}^d\mathbf{R}_S d\Omega$; $\mathbf{v}_{e2}^o = \int_{\Omega e}\mathbf{R}_S^T\boldsymbol{\varepsilon}^o d\Omega$; $\mathbf{G}_{e2} = \int_{\Omega e}\mathbf{B}^T\mathbf{R}_R d\Omega$

The variational Eq. (28) with respect to $\mathbf{h}_{e1}$

$$\mathbf{F}_{e1}\mathbf{h}_{e1} + \mathbf{F}_{e12}\mathbf{h}_2 + \mathbf{v}_{e1}^o - \mathbf{G}_{e1}^T\mathbf{q} = \mathbf{0} \quad \forall e \in S \tag{29}$$

- *In all elements of the structure*

The variational Eq. (15b) with respect to $\mathbf{q}$ restores the equilibrium equation of the structure and taking account of Eqs. (22) and (28)

$$\sum_{e \in R}\mathbf{g}_e + \sum_{e \in S}\mathbf{g}_e = \mathbf{0} \tag{30}$$

$$\text{Where } \begin{matrix} \mathbf{g}_e = \mathbf{G}_{e1}\mathbf{h}_{e1} & \forall e \in R \quad (a) \\ \mathbf{g}_e = \mathbf{G}_{e1}\mathbf{h}_{e1} + \mathbf{G}_{e2}\mathbf{h}_2 & \forall e \in S \quad (b) \end{matrix} \tag{31}$$

Replace $\mathbf{h}_{e1}$ from Eq. (29) into Eq. (31b), the expression of $\mathbf{g}_e$ is following

$$\mathbf{g}_e = \mathbf{K}_e\mathbf{q} + \mathbf{G}^*_{e2}\mathbf{h}_2 - \mathbf{g}^o_e \quad \forall e \in S \tag{32}$$

Where $\mathbf{G}^*_{e2} = \mathbf{G}_{e2} - \mathbf{G}_{e1}\mathbf{F}^{-1}_{e1}\mathbf{F}_{e12}$

Replacing Eqs. (25) and (32) into Eq. (30) gives

$$\mathbf{K}\mathbf{q} + \mathbf{G}^*_2\mathbf{h}_2 = \mathbf{g}^o \tag{33}$$

Where $\mathbf{K} = \sum_{e \in E} \mathbf{K}_e$; $\mathbf{g}^o = \sum_{e \in E} \mathbf{g}^o_e$; $\mathbf{G}^*_2 = \sum_{e \in S} \mathbf{G}^*_{e2}$

The variational Eq. (28) with respect to $\mathbf{h}_2$ gives

$$-\mathbf{G}^{*T}_2\mathbf{q} - \mathbf{F}^*_2\mathbf{h}_2 = \mathbf{v}^{o*}_2 \tag{34}$$

Where $\mathbf{F}^*_2 = \sum_{e \in S} \mathbf{F}^T_{e12}\mathbf{F}^{-1}_{e1}\mathbf{F}_{e12} - \mathbf{F}_{e2}$; $\mathbf{v}^{o*}_2 = \sum_{e \in S} \mathbf{F}^T_{e12}\mathbf{F}^{-1}_{e1}\mathbf{v}^o_{e1} - \mathbf{v}^o_{e2}$

The equation systems (33) and (34) can be written in the form

$$\tilde{\mathbf{K}}\tilde{\mathbf{q}} = \tilde{\mathbf{g}} \tag{35}$$

Where $\tilde{\mathbf{K}} = \begin{bmatrix} \mathbf{K} & \mathbf{G}^*_2 \\ -\mathbf{G}^{*T}_2 & -\mathbf{F}^*_2 \end{bmatrix}$; $\tilde{\mathbf{q}}^T = [\mathbf{q}^T, \mathbf{h}^T_2]$; $\tilde{\mathbf{g}} = \begin{bmatrix} \mathbf{g}^o \\ \mathbf{v}^{o*}_2 \end{bmatrix}$

Solving of the equation system (35) will provide unknown displacements $\mathbf{q}$ at the nodes and the singular stress parameters $\mathbf{h}_2$. After that the stress intensity factors can be obtained by the formula (Fleury *et al.* 1994)

$$\begin{aligned} K_i = \sqrt{2\pi}\Bigg\{ he_1\left[\mathrm{Re}\left(\sum_{m=1}^{3} C_{m,1} r_{i,m}\right) + \mathrm{Im}\left(\sum_{m=1}^{3} C_{m+3,1}\bar{r}_{i,m}\right)\right] + \\ + he_2\mathrm{Re}\left(\sum_{m=1}^{3} C_{m,2} r_{i,m} + C_{m+3,2}\bar{r}_{i,m}\right) + he_3\mathrm{Im}\left(\sum_{m=1}^{3} C_{m,3} r_{i,m} + C_{m+3,3}\bar{r}_{i,m}\right)\Bigg\} \end{aligned} \tag{36}$$

With $i = 2, 4, 6$ ($K_2 = K_I$, $K_4 = K_{III}$, $K_6 = K_{II}$) and $r_{6,m}$ at here is $r_{3,m}$ in Eq. (12).

The components of strain energy release rate were calculated by using forces and displacements near the crack tip with Irwin's virtual crack closure technique as Raju *et al.* (1988)

$$G_I = \frac{1}{\Delta 2}[F_{yi}\{t_{11}(v_m - v'_m) + t_{12}(v_k - v'_k)\} + F_{yj}\{t_{21}(v_m - v'_m) + t_{22}(v_k - v'_k)\}] \tag{37}$$

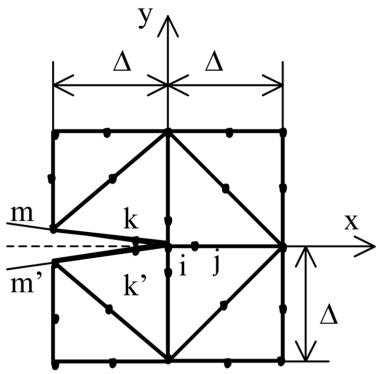

Fig. 2 Nodes used in G calculations

Where F_{yi} is the force in the y direction at node i, v_m is the displacement at node m, etc. (see Fig. 2). The values of t_{ij} are constants given in Raju *et al*. (1988).

Similar, the expressions for G_{II} and G_{III} were used with F_y replaced by F_x and F_z and v replaced by u and w, respectively. The total strain energy release rate, G, is calculated by the formula

$$G = G_{II} + G_{II} + G_{III}$$

4. Numerical results

We consider four-layer symmetric laminates $[+\theta/-\theta]_s$ with the same thickness $h = 1$ (in) and with the material properties as in Byron and Pagano (1970): $E_3 = 20 \times 10^6$ (psi), $E_1 = E_2 = 2.1 \times 10^6$ (psi), $G_{12} = G_{23} = G_{31} = 0.85 \times 10^6$ (psi), $\nu_{12} = \nu_{32} = \nu_{31} = 0.21$. The distance between the pair of free edges is $2b = 16\ h$. We consider the laminates in the two cases

- Problem of free edge interlaminar stresses (before delamination) under extension and under bending;
- Delamination under extension and under bending.

For the case of uniform axial extension, we have: $\varepsilon_3^o = e$ = constant, $K_3 = X_3 = K_5 = 0$. For the case of bending, we have: $K_3 = 1/h$, $\varepsilon_3^o = X_3 = K_5 = 0$.

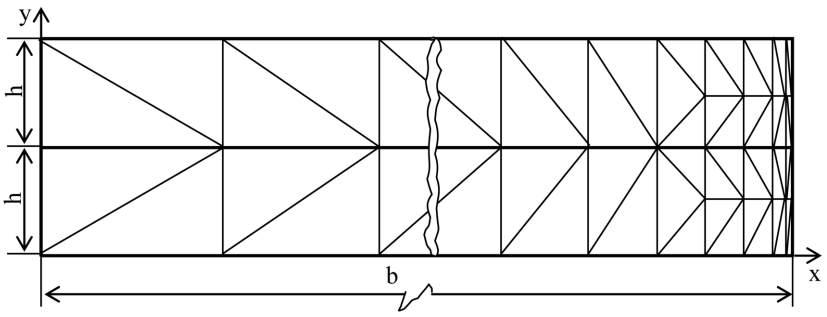

Fig 3 Mesh of the quarter of the cross section of laminate

4.1 Free-edge interlaminar stresses

Condider the composite laminate $[+45^o/-45^o]_s$

- For the case of uniform axial extension: In this case due to material and geometric symmetry conditions, only a quarter of the cross section of laminate ($x \geq 0$ and $y \geq 0$) is considered. The second-degree triangular element and a mesh of 236 elements and 525 nodes with the refinement growing towards the free edge are used (Fig. 3).
- For the case of bending: In this case due to material and geometric symmetry conditions permit that only one half of the cross section of laminate with 472 elements and 1009 nodes (2 times of the mesh in the Fig. 3 with $x \geq 0$ and $-2h \leq y \leq 2h$) be examined.

In two cases (extension and bending), since the distribution of stress components are anti-symmetric or symmetric, we only need to discuss the stress distribution in a quarter region ($x \geq 0$ and $y \geq 0$).

In this paper we will only compare present results with those of other methods in the case of bending because for the case of extension, results were compared with those of the literature. It showed that the results of the present method in the case of extension are very good (Nguyen, T.D. and Nguyen, D.H. in press). Now, the results in the case of extension are compared with those in the case of bending.

The distribution of the interlaminar normal stress σ_y at $y = h$ for the case of bending is presented in the Fig. 4.

The Fig. 4 shows that the stress σ_y presents a compressive behavior near free edge. By the anti-symmetry of deformation, σ_y is tensional in the interface $y = -h$ near free edge. The present results are similar with those of Ye (1990) and Cho and Kim (2000) in all region except near free edge. At free edge, the difference between the solutions is very important. The absolute value of σ_y at the corner of the interface $y = h$ and $x = b$ in the solution of Davì and Milazzo (1999) is very high in comparison with the present solution and also with other solutions. The present result at this corner is much agreement with that of Cho and Kim (2000).

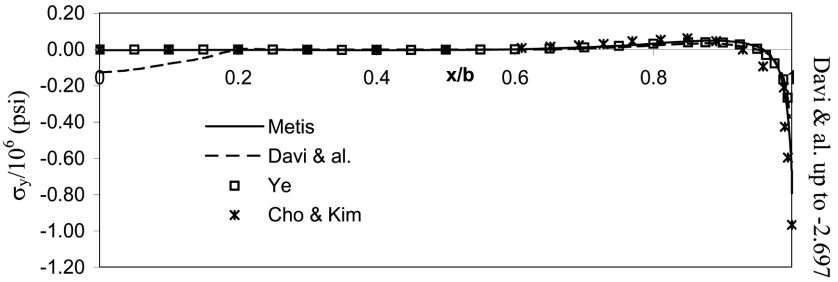

Fig. 4 Normal stress σ_y at $y = h$ in the case of bending

Table 1 Stresses at the corner of $y = h$ and $x = b$ (in 10^6 Psi)

Author	Method used	σ_y	τ_{xy}	τ_{yz}
Present	Metis	−0.793	1.75×10^{-6}	1.91
Davì and Milazzo (1999)	Boundary element	−2.697		3.073
Ye (1990)	Heterogeneous model	−0.266		1.947
Cho and Kim (2000)	Iterative method	−0.966	0	2.258

The Fig. 5 presents the distribution of the normal stress σ_y at $y = h$ for the two cases (extension and bending) calculated by present method. It is seen that σ_y for the case of bending is close to that for the case of extension.

The Fig. 6 presents the distribution of the interlaminar shear stress τ_{xy} at the interface $y = h$ for two cases. In the case of bending, the values of τ_{xy} in the solution of Cho and Kim (2000) are always greater than those in the present solution. The form of the two curves is similar, they increase and have a tip near free edge then they decrease very sharply to zero at $x = b$. For laminate $[+45^o/-45^o]_s$, the stress τ_{xy} in the case of bending is different with that in the case of extension. The stress τ_{xy} in the case of extension is very small in comparison with that in the case of bending. The present results of stress τ_{xy} under extension are very close to those of Tian *et al.* (2004) used three-

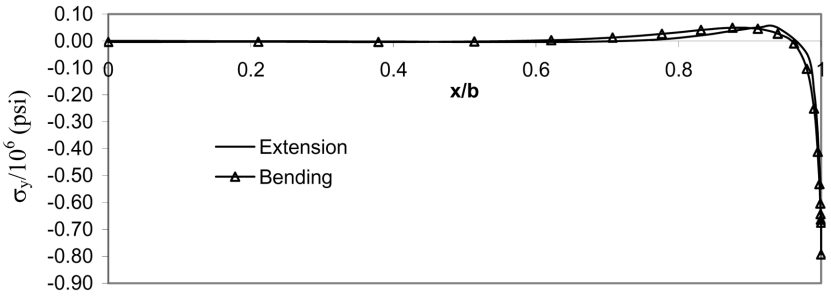

Fig. 5 Normal stress σ_y at $y = h$ in the two cases

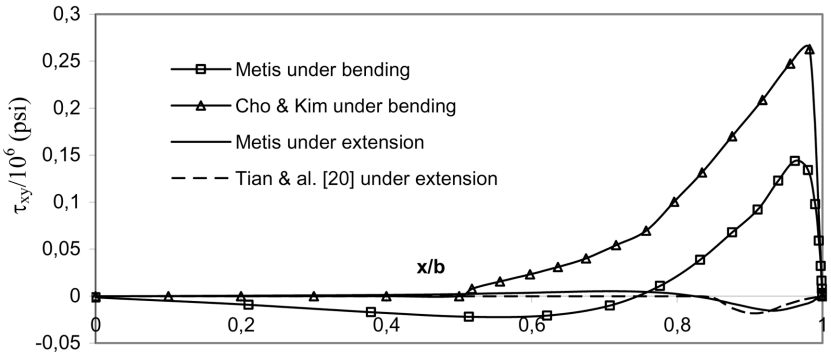

Fig. 6(a) Interlaminar shear stress τ_{xy} at $y = h$ in the two cases for $[+45^o/-45^o]_s$

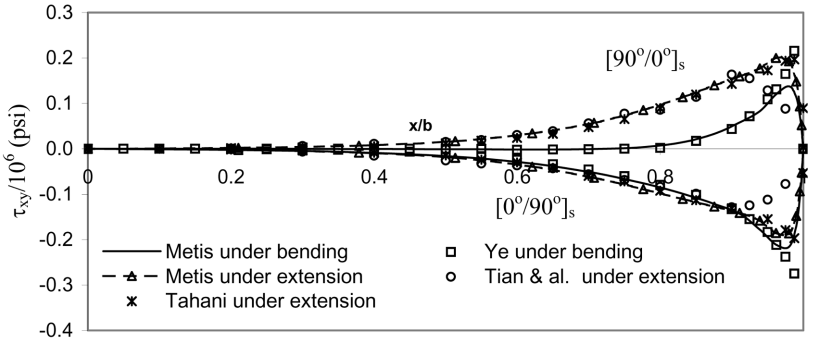

Fig. 6(b) Interlaminar shear stress τ_{xy} at $y = h$ for $[90^o/0^o]_s$ and $[0^o/90^o]_s$

dimensional hybrid stress element.

For laminate $[90^o/0^o]_s$, there is a difference of the stress τ_{xy} between the case of bending and that of extension (see Fig. 6b). For laminate $[0^o/90^o]_s$, the stress τ_{xy} in the case of bending is similar to that in the case of extension. In the case bending, the present results are agreement with those of Ye (Ye 1990) except near free edge. Near free edge, the peak stress values of τ_{xy} of Ye (1990) are more important than those of present method. In the case of extension, the present result of τ_{xy} is excellent agreement with that of Tahani and Nosier (2003) used layerwise theory. These results are higher than those of Tian *et al.* (2004). In general, it is noticed that the stress τ_{xy} in the case of bending is different with that in the case of extension.

The distribution of the interlaminar stress τ_{yz} along the interface $y = h$ for the case of bending is shown in the Fig. 7. The stress τ_{yz} increases rapidly near free edge. This indicates that τ_{yz} has a significant stress concentration near free edge. The present results are quite good agreement with those of Davì and Milazzo (1999) and of Ye (1990) with some discrepancies in the region near free edge. These results are greater than those of Cho and Kim (2000). At free edge, the value of τ_{yz} in present method is close to that of Ye (1990) (see Table 1), it is very important in the solution of Davì and Milazzo (1999).

The Fig. 8 shows the distribution of the interlaminar shear stress τ_{yz} at the interface $y = h$ for the cases of extension and of bending. It is found that the stress τ_{yz} in the two cases is similar.

The Fig. 9 is the through-thickness distribution of the shear stress τ_{yz} in the two cases. The values of shear stress τ_{yz} in the both cases attain the maximum at the interface $y = h$. Shear stresses τ_{yz} in the two cases increase from the upper surface and mid-plane. Particularity, neighborhood of the interface $y = h$, they increase very suddenly. In the case of bending, the present result is much closed to that of Ye (1990).

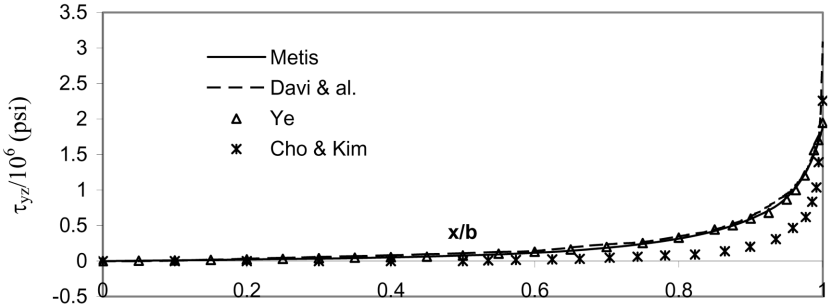

Fig. 7 Interlaminar shear stress τ_{yz} at $y = h$ in the case of bending

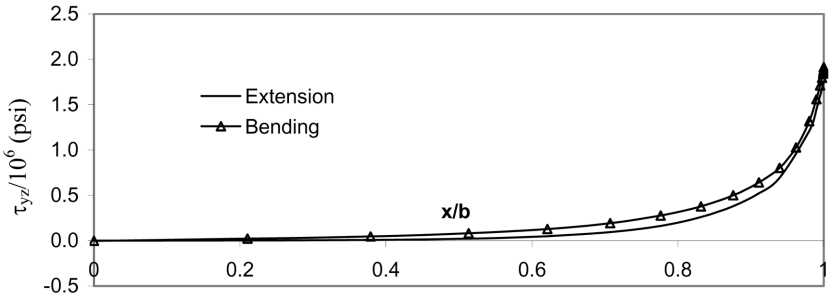

Fig. 8 Interlaminar shear stress τ_{yz} at $y = h$ in the two cases

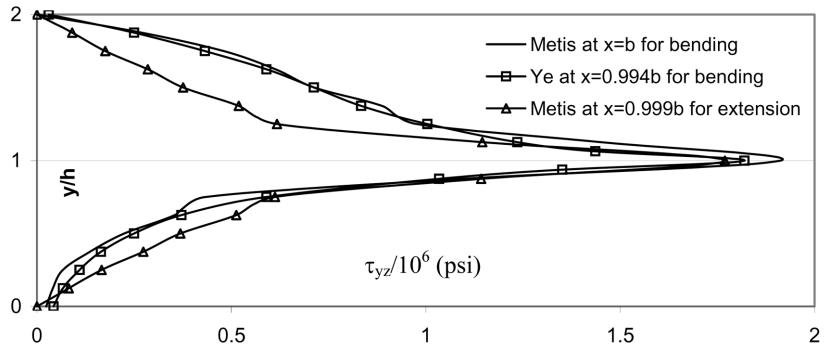

Fig. 9 Through-thickness distribution of shear stress τ_{yz} in the two cases

4.2 Delamination in composite laminates

In this section, we consider a composite laminate $[+\theta/-\theta]_s$ with the material and geometric properties as the previous example. The crack length is a = 1 in.

4.2.1 Delamination under uniform axial extension

The laminate subjects to a uniform axial extension $\varepsilon_3^o = e$ = constant. Second-degree triangular elements and a mesh of 56 elements for a quarter of the cross section of laminate are used (Fig. 10).

The results of stress intensity factors K_i (I = I, II, III) for various fiber orientations of $\pm\theta$ degrees are presented in the Fig. 11.

It is seen that the K_{III} is always clearly dominant. This tearing mode corresponds to a shearing out of plan, due to the interlaminar shear stress τ_{yz}. The K_I is also significant. It is due to the interlaminar normal stress σ_y. The K_{II}, due to the interlaminar shear stress τ_{xy}, is always very weak. We also note that when the angles of the fibers $|\pm\theta|$ are grater than 60 degrees, the three modes are simultaneously cancelled.

The Figs. 12, 13 and 14 indicate that present results and those of Wang (1984) and of Qian and Sun (1997) are identical in K_{III}. There are substantial different in K_I and K_{II} between present results and those of Wang (1984) and of Qian and Sun (1997) and also between the results of Wang (1984) and those of Qian and Sun (1997), in the magnitude and in the sign. Qian and Sun (1997) explained that this difference is caused by the difference of the near-tip crack surface relative displacement

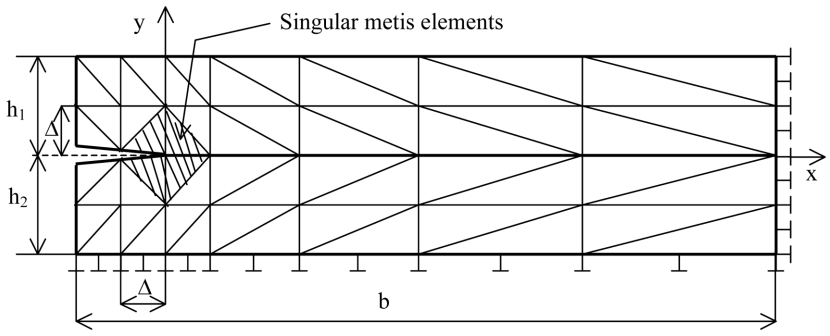

Fig. 10 Delamination of laminates under extension

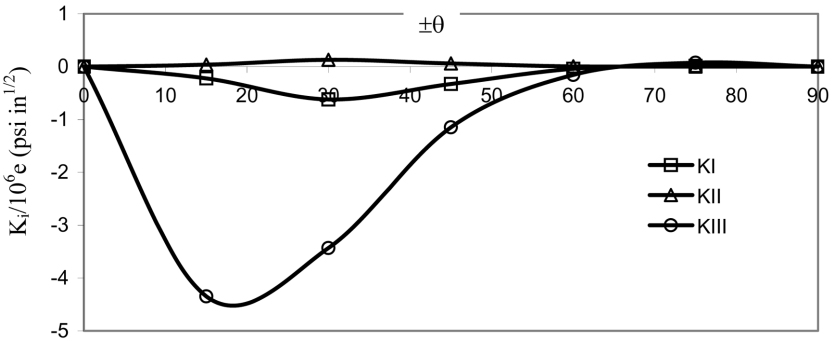

Fig. 11 Stress intensity factor K_i of laminates under extension

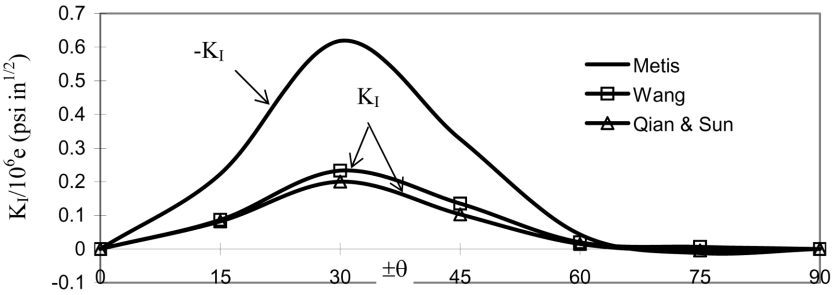

Fig. 12 Stress intensity factor K_I of laminates under extension

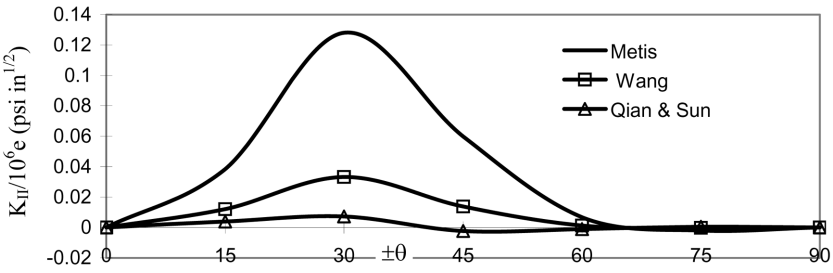

Fig. 13 Stress intensity factor K_{II} of laminates under extension

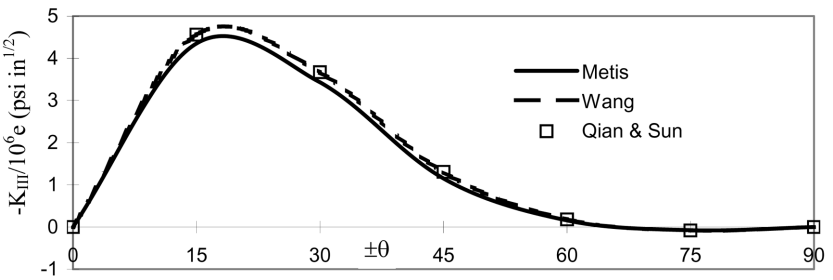

Fig. 14 Stress intensity factor K_{III} of laminates under extension

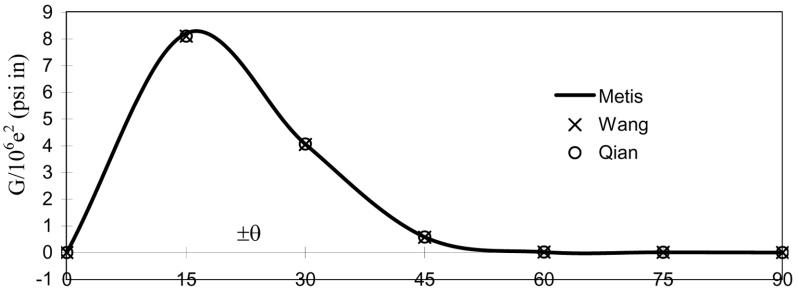

Fig. 15 Total strain energy release rate G of laminates under extension

between these methods.

In the present result, K_I is always negative when $|\pm\theta| \le 60^\circ$. There is a tendency of crack closing in this mode when $|\pm\theta| \le 60^\circ$. When we change the direction of load, it means that the structure is subjected to axial compression ($\varepsilon_z = -e$), we found that K_I, K_{II} and K_{III} have the same magnitudes with the case $\varepsilon_z = e$ but their sign is changed. K_I becomes positive when $|\pm\theta| \le 60^\circ$. So in the case of $\varepsilon_z < 0$ and $|\pm\theta| \le 60^\circ$, the propagation of three modes simultaneously exist.

The maximum value of the K_{III} is about six and thirty times higher than that of K_I and K_{II}, respectively. Therefore the difference of K_I and of K_{II} in the present solution with the solution of Wang and of Qian may not significantly influence the structural analysis.

The total strain energy release rate G for various fiber orientations of $\pm\theta$ degrees is shown in Fig. 15. The results show that the energy release rate is highest for a composite laminate $[\pm\theta]_s$ with $\theta = 16^\circ$ and has the small value with $\theta \ge 45^\circ$. The total strain energy release rate of present method is very close to that of Wang (1984) and of Qian and Sun (1997).

4.2.2 Delamination of composite laminates under bending

The laminate subjects to a bending $K_3 = 1/h$. The second-degree triangular elements and a mesh of 56 elements for one half of the cross section of laminate are considered (Fig. 16).

The stress intensity factors K_i ($i = I, II, III$) for the two cracks are presented in Figs. 17 and 18. As the case of delamination under extension, in this case of K_{III} is dominant; K_I is significant; K_{II} is

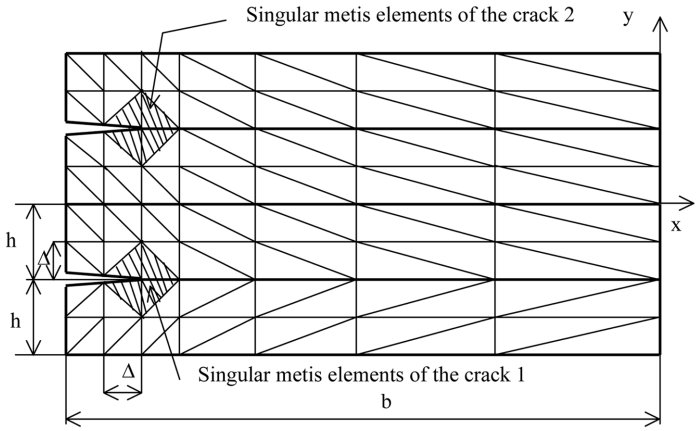

Fig. 16 Delamination of laminates under bending

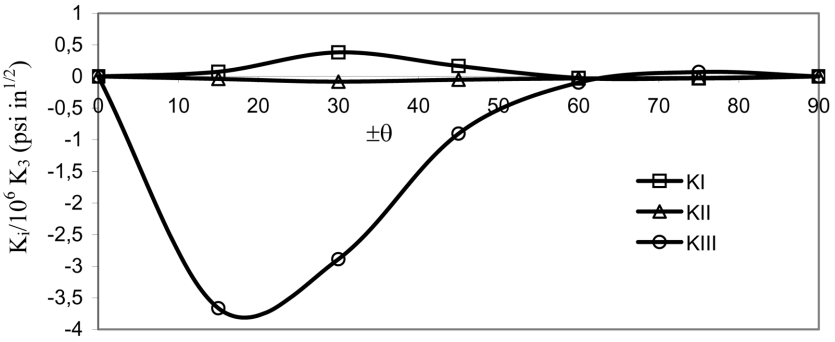

Fig. 17 Stress intensity factor K_i of the crack 1 under bending

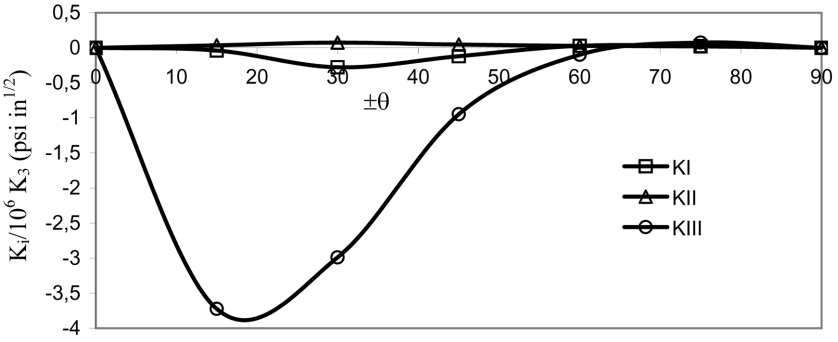

Fig. 18 Stress intensity factor K_i of the crack 2 under bending

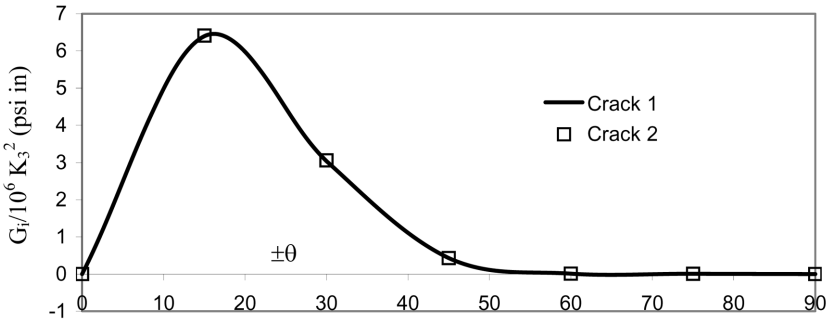

Fig. 19 Total strain energy release rate G under bending

very weak. When θ is ±60 degrees, the three modes are simultaneously cancelled. For the crack 1, K_I is positive when $|\theta| < 60^o$, so the delamination propagation in the mode I can happen. For the crack 2, K_I is negative when $|\theta| < 60^o$, so the delamination propagation in the mode I doesn't happen.

We find that in the case of bending, the stress intensity factors K_i of the crack 2 in the part of the laminate subjected to axial extension are similar to those for the axial extension (see Figs. 11 and 18).

The total strain energy release rate G for various fiber orientations of $\pm\theta$ degrees of composite laminates under bending is shown in Fig. 19. As laminates under extension, the energy release rate is highest for a composite laminate $[\pm\theta]_s$ with $\theta = 16^o$ and has the small value with $|\theta| \geq 45^o$. The total strain energy release rate of the two cracks (crack 1 and crack 2) is similar.

5. Conclusions

For the problem of free edge interlaminar stresses: The distribution of interlaminar stresses under bending in the part of laminate subjected to extension has the characteristics similar to those in the laminate under uniform axial extension except for the interlaminar shear stress τ_{xy}.

For the problem of delamination of composite laminates: The stress intensity factor and the strain energy release rate under bending in the part of the laminate under extension are similar to those in the laminate under uniform axial extension.

After some numerical tests for laminates under extension and under bending, it appears that the metis element method constitutes a very effective tool to calculate the interlaminar stresses for the problem of free edge composite laminates, the stress intensity factors and the strain energy release rate for the problem of delamination in composite laminates.

References

Byron, R. and Pagano, N.J. (1970), "Interlaminar stresses in composite laminates under uniform axial extension", *J. Compos. Mater.*, **4**, 538-548.

Cho, Maenghyo and Kim, Heung Soo (2000), "Iteractive free-edge stress analysis of composite laminates under extension, bending, twisting and thermal loadings", *Int. J. Solids Struct.*, **37**, 435-459.

Davì, G. and Milazzo, A. (1999), "Bending stress fields in composite laminate beams by a boundary integral formulation", *Comput. Struct.*, **71**, 267-276.

De Saxce, G. (1992), "Conception d'un élément fini hybride métis monocouche pour la modélisation du delaminage dans les matériaux composites", rapport interne du service M.M.S. de la F.P.Ms, Projet Multimatériaux, October 1992.

De Saxcé, G. and Kang, C.H. (1992), "Application of the hybrid mongrel displacement finite element method to computation of stress intensity factors in anisotropic material", January, **41**(1), 71-83.

Fleury, C., Nguyen, D.H., Guerlement, G. and Fryns, G. (1994), "Développement et validation de modèles pour la caractérisation des propriétés mécaniques et la description des mécanismes d'endommagement de structures en matériaux composites", Rapport SF-193, Université de Liège.

Kang, Chi-Hang (1991), "Une famille d'éléments hybrides singuliers pour l'étude des plaques fissurées métalliques et composites", Thèse de doctorat, Université de Technologie de Compiègne.

Kim, K.S. and Hong, C.S. (1985), "Characteristics of free edge delamination in angle-ply laminate", *Fifth International Conference on Composite Materials ICCM-V*, July 29 – August 1, 347-361.

Lekhnitskii, S.G. (1963), "Theory of elasticity of an anisotropic body", holden-day, San/Fransco, California, USA.

Nguyen, Dang Hung (1978), "On the monotony and the convergence of a special class of hybrid finite element: the mongrel element", *Variational Methods in Mechanics of Solids* (Ed. by S. Nemat-Nasser), Pergamon.

Nguyen, Dang Hung and Tran, Thanh Ngoc (2004), "Analysis of cracked plates and shells using "metis" finite element model", *Finite Elem. Anal. Des. (Elsevier)*, **40**, 855-878.

Nguyen, Dang Hung, De Saxcé, G. and Kang, C.H. (1991), "The computation of 2-D stress intensity factors using a hybrid mongrel displacement finite elements", *Eng. Fract. Mech.*, **38**, 197-205.

Nguyen, Dang Hung, Tran, Thanh Ngoc and Nguyen, Tai Trung (2002), "Analysis of uncracked and cracked plate bending problem using metis finite element model", *Proc. 7th Nat. Congr. On Mech.*, Hanoi, December 18-20, 262-270.

Nguyen, Tien Duong and Nguyen, Dang Hung (2004), "Calculation of free edge stress for composite laminates by metis element method", International Conference: Mécanique pour l'Ingénieur 2004 – Ho Chi Minh City Vietnam August 16-20.

Nguyen, Tien Duong and Nguyen, Dang Hung (2004), "Using metis model to solve torsion problem of prismatic bar", *The 7th National Congress on Deformation Solid Mechanics – Do Son*, Vietnam 27-28 August 2004.

Nguyen, Tien Duong and Nguyen, Dang Hung, "Computation of interlaminar stresses using Metis elements", submitted to the Journal "Struct. Eng. Mech.".
Nguyen, Tien Duong and Nguyen, Dang Hung, "Direct and indirect metis element methods for edge delamination in laminates", Paper N° 317, COMPUTATIONAL MECHANICS WCCM VI in Conjunction with APCOM'04, *Sept. 5-10, 2004, Beijing, China* © 2004 Tsinghua University Press & Springer-Verlag.
Qian, W. and Sun, C.T. (1997), "Calculation of stress intensity factors for interlaminar cracks in composite laminates", *Compos. Sci. Technol.*, **57**, 637-650.
Raju, I.S., Crews, J.H. and Aminpour, M.A. (1988), "Convergence of strain energy release rate components for edge-delaminated composite laminates", *Eng. Fract. Mech.*, **30**(3), 383-396.
Rotem, A. and Hashin, Z. (1975), "Faillure modes of angle ply laminates", *J. Compos. Mater.*, **9**, 191-206.
Tahani, Masoud and Nosier, Asghar (2003), "Three-dimensional interlaminar stress analysis at free edges of general cross-ply composite laminates", *Mater. Design,* **24**, 121-130.
Tian, Zongshu, Zhao, Fengdong and Yang, Qingping (2004), "Straight free-edge effects in laminated composites", *Finite Elem. Anal. Des.*, **41**, 1-14.
Wang, S.S. (1984), "Edge delamination in angle-ply composite laminates", *A.I.A.A. J.*, **22**, 256-264.
Ye, Lin (1990), "Some characteristics of distributions of free-edge interlaminar stresses in composite laminates", *Int. J. Solids Struct.*, **26**, 331-351.

Notation

$\mathbf{C}_m$	: Eigen coefficients
def	: Partial derivative operator of "strain"
$e(x, y)$	: Axial strain which is independent of the z axis
equ	: Partial derivative operator of "equilibrium"
$\mathbf{F}(x, y)$	: Airy's stress function
$\mathbf{g}_e$	: Generalized force of each element
$\mathbf{h}_{e1}$	: Vector of unknown parameters of regular part of discretisation stress field
$\mathbf{h}_{e2}$	: The vector of unknown parameters of singular part of discretisation stress field
Inf	: Minimum of the function $\prod(\sigma, u)$
K_3	: Bending curvature in the weak inertia plan Oyz
K_5	: Warping angle about z-axis
L_2, L_3 et L_4	: Derivative operators in order 2, 3 and 4, respectively
$\mathbf{N}(x)$	: Shape function matrix of the displacement field
$\mathbf{q}$	: Nodal displacement vector
$\mathrm{Re}(\delta)$	: Real part of δ
$\mathbf{R}_R(x)$	: Polygonal interpolation matrix of regular part of discretisation stress field
$\mathbf{R}_S(x)$	: Singular matrix of singular part of discretisation stress field
S_i	: Interface between two contiguous elements
S_{ij}	: Compliance tensor (i, j = 1, 2, 3, 4, 5, 6)
$S^d_{\alpha\beta}$	: Reduced compliance tensor of S_{ij} (α, β = 1, 2, 4, 5, 6)
$\mathrm{Sup}\ \prod(\sigma, u)$	: Maximum of the function $\prod(\sigma, u)$
$\mathbf{t}(\boldsymbol{\sigma})$	: Tension on the boundary Ω
$\mathbf{u}^{3D}$	: Displacement field in 3 dimensions
u^{3D}, v^{3D}, w^{3D}	: Components of displacement field in 3 dimensions
$W(\boldsymbol{\sigma})$	: Complementary strain energy density
X_3	: Bending curvature in the strong inertia plan Oxz
z_m	: Generalized complex variable
δ	: Stress singularity order
$\boldsymbol{\varepsilon}$	: Strain field
$\boldsymbol{\sigma}$	: Stress field
Π	: Total complementary strain energy

Π_e : Complementary strain energy of the element e
μ_m : Roots of the characteristic equation
Ω : Section of the structure
Ω_e : Section of the element
$\boldsymbol{\varepsilon}^o$: Vector of the imposed initial strains
$\partial\Omega$: Boundary of the section Ω
$\Psi(x, y)$: Prandtl's stress function
ε_3^o : Mean strain